CHEMICAL ENGINEERING TRANSACTIONS
VOL. 117, 2025
A publication of AIDIC
The Italian Association of Chemical Engineering
Online at www.cetjournal.it
Guest Editors: Fabrizio Bezzo, Flavio Manenti, Gabriele Pannocchia, Almerinda di Benedetto

ISBN 979-12-81206-17-5; **ISSN** 2283-9216
DOI: 10.3303/CET25117132

Discrete Element Method Study on Spreading Behaviour of Non-spherical Polymeric Powder in Powder Bed Fusion with Blade and Roller Spreaders

Sina Zinatlou Ajabshir [a,b], Colin Hare[b], Diego Barletta[a], Massimo Poletto[a]

[a] Department of Industrial Engineering, University of Salerno, Via Giovanni Paolo II, 132, 84084 Fisciano, SA, Italy
[b] School of Engineering, Newcastle University, Newcastle upon Tyne NE1 7RU, UK
sizinatlouajabshir@unisa.it

The properties of the spread powder layer are key in Powder Bed Fusion (PBF) additive manufacturing. Higher packing density and a uniform powder layer are vital for part quality. This study examined the impact of blade-shaped and roller-shaped spreading tools on powder behaviour using the Discrete Element Method (DEM). Switching from a blade to a roller at a spreading speed of 30 mm/s improved the packing fraction by 76% and reduced surface roughness by 16%. The roller-shaped tool produced a more effective initial powder layer with a better packing fraction and a smoother surface finish.

1. Introduction

PBF is a powder-based additive manufacturing process where the powder is transferred from a fresh powder source to the fusion bed using a spreading tool. The powder is selectively fused based on a predefined CAD file, followed by the spreading of a new powder layer on top, and this process repeats until the final 3D component is manufactured (Mohammadkamal and Caiazzo, 2025). The uniformity and packing density of the powder spread on the fusion bed directly impact the quality of the final component, influencing the formation of microscopic defects and dimensional accuracy (Tang et al., 2023), residual stresses (Mohammadkamal and Caiazzo, 2024) and mechanical properties (Sofia et al., 2019). These factors are influenced by the physical properties of the powder, including particle size (He et al., 2021; Yao et al., 2022), morphology (Yim et al., 2022) and size distribution (Zhao and Chew, 2021), as well as process parameters like spreading tool speed (Lupo et al., 2023; Nan and Gu, 2022), tool geometry (Horn et al., 2024; Phua et al., 2021), and environmental conditions like humidity (Cordova et al., 2020) and temperature (Zinatlou Ajabshir et al., 2024a, 2024b). The geometry of the spreading tool significantly affects the uniformity and density of spread powders (Chen et al., 2020), making it essential to evaluate its impact (Wang et al., 2021). The geometry of the spreading tool remains a topic of debate. The above studies primarily utilised spherical particles. However, the spreading and flow behaviour of irregularly shaped particles in PBF remains underexplored, particularly regarding the influence of different tool geometries. This understanding of powder behaviour is achievable through precise modelling and analysis. The Discrete Element Method (DEM) is a powerful simulation technique for studying particle interactions in detail (Lupo et al., 2019). In PBF, DEM helps analyse how powder particles spread, pack, and interact during the process (Lupo et al., 2024). Investigating these dynamics through DEM simulations provides precise microscale measurements that are difficult to achieve experimentally. DEM offers a cost-effective alternative to repeated experiments and accurately replicates particle shapes, providing insights and technical support to improve powder spreading in PBF.

This study uses DEM to examine the spreading behaviour of polyamide 6 (PA6), a polymeric powder with non-spherical and highly irregular particle morphology, using two spreading tool geometries. The tools analysed include a blade-shaped tool and a roller-shaped tool. The particle shapes were modelled by replicating clumped particles using a multi-sphere approach in DEM simulations. The dynamic behaviour and performance of each tool, particularly in terms of spread powder packing fraction and surface roughness, were evaluated to provide

Paper Received: 15 January 2025; Revised: 5 March 2025; Accepted: 22 May 2025
Please cite this article as: Zinatlou Ajabshir S., Hare C., Barletta D., Poletto M., 2025, Discrete Element Method Study on Spreading Behaviour of Non-spherical Polymeric Powder in Powder Bed Fusion with Blade and Roller Spreaders, Chemical Engineering Transactions, 117, 787-792 DOI:10.3303/CET25117132

insight into their influence on the spreading process. The findings aim to establish whether different geometries impact the powder layer's quality and to identify the underlying mechanisms of these effects.

2. Methodology

2.1 Materials

This study uses PA6 particles to replicate particle behaviour during the spreading phase in PBF. The PA6 particles have characteristic sizes of 15 µm, 46 µm, and 91 µm, representing the 10th, 50th, and 90th percentiles, respectively. For simulations, particle sizes were scaled by a factor of 43, ranging from 0.65 mm to 4 mm, with a mean size of 2 mm, matching the real powder's distribution. To accurately simulate particle behaviour, irregular particle shapes were modelled, as shown in Figure 1a. The overlapping multi-sphere method (Favier et al., 1999) was used to represent complex shapes efficiently, with elongated clumps selected to balance accuracy and computational time based on the previous work (Zinatlou Ajabshir et al., 2024a). This approach ensures a reliable depiction of particle behaviour during spreading.

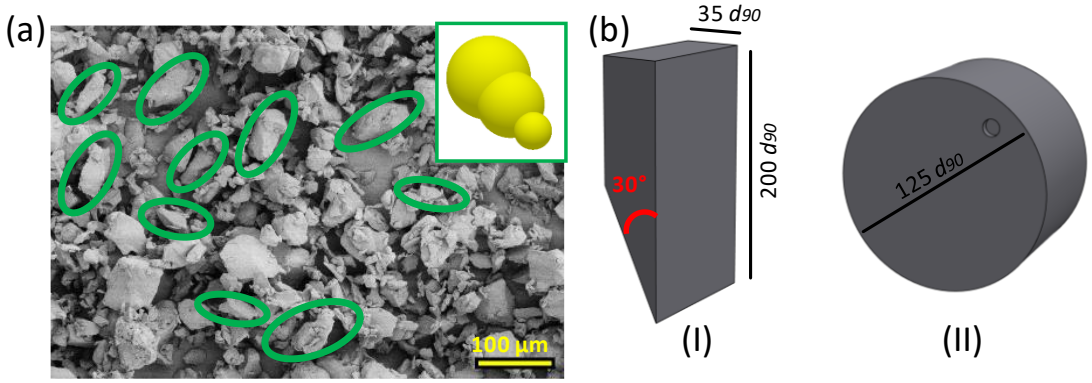

Figure 1: (a) SEM images of the PA6 powder morphology along with the elongated particle shape used in simulation; (b) geometry of the spreading tools: (I) blade-shaped and (II) roller-shaped where each one has 40d_{90} width.

2.2 DEM model and powder spreading simulation

The spreading process was simulated in Altair EDEM2022 using an already calibrated and validated DEM model (Zinatlou Ajabshir et al., 2024a). The simulation employed the Hertz–Mindlin (Hertz, 1881; Mindlin, 1949; Mindlin and Deresiewicz, 1989) model and the JKR cohesive model (Johnson et al., 1971) to describe interparticle forces, leveraging GPU acceleration for efficiency. Table 1 shows the particle and geometry properties and their interaction parameters. To reduce computational costs and optimize the simulation time step, Young's modulus was scaled down by 3 orders of magnitude (divided by 1000), and the cohesion was adjusted accordingly to maintain the same value of the dimensionless cohesion number, Coh (Behjani et al., 2017; Zinatlou Ajabshir et al., 2024a).

Table 1: Summary of the material properties and interaction parameters (Zinatlou Ajabshir et al., 2024a)

Parameters	Value (P: Powder & G: Geometry)
Powder density (kg/m^3)	P: 1130, G: 8000
Poisson's ratio	P: 0.35, G: 0.33
Young's modulus (GPa)	P: 0.0034, G: 193
Surface energy (mJ/m2)	P: 94, G: -
Coefficient of sliding friction	P_P: 0.639, G_P: 0.53
Coefficient of restitution	P_P: 0.5, G_P: 0.5
Coefficient of rolling friction	P_P: 0.001, G_P: 0.0001

The spreading simulation used 300,000 particles generated by a dynamic factory, creating a settled powder bed in front of the spreading tool. This powder pile, shown in Figure 2, served as the initial condition. The simulation domain was periodic in the X direction, perpendicular to the spreading path (Y direction), with a width of about 15 times the particle diameter (d_{90}). The total bed length was 650 d_{90}, with a focus on an analysis area of 300 d_{90} in length. The gap (δ) between the spreading tool and the base plate was set to approximately 3 d_{90}. A

spreading speed of 30 mm/s was selected to match the experimental conditions on which the model had been previously fully validated (Zinatlou Ajabshir et al., 2024b).

2.3 Analysis procedure

The simulated powder layer was visually analysed by normalizing the particle height in the Z direction to the gap size (h/δ).
The powder bed quality was evaluated by analysing the packing fraction. The bed from the spreading simulation was divided into 75 bins along the spreading direction. Each bin had a length of $4d_{90}$, a height equal to the powder bed depth (gap size), and the same width as the domain. The packing fraction was then calculated as Eq(1):

$$Packing\ fraction\ in\ each\ bin\ = \frac{Total\ particle\ volume\ in\ the\ bin}{Volume\ of\ the\ bin} \quad (1)$$

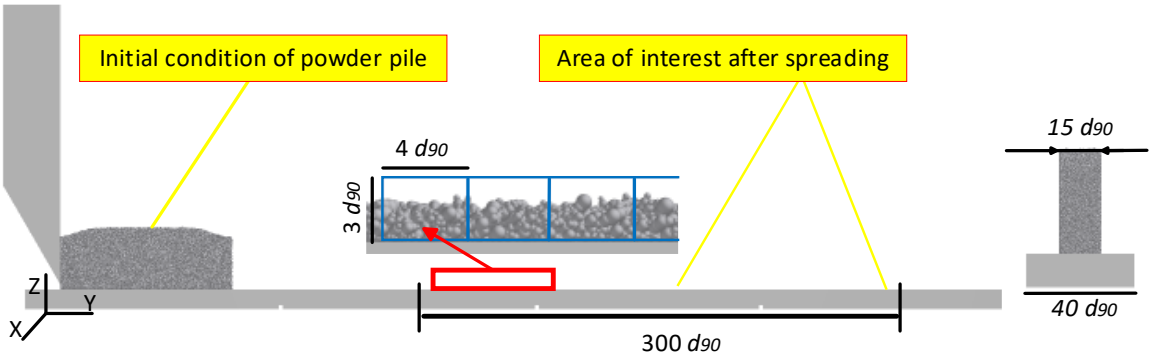

Figure 2: Powder spreading set up in the simulation, highlighting the studied area for the surface quality and the packing fraction.

The surface roughness of the powder bed cross-section was analysed by developing a MATLAB code that utilized image processing and quantitative evaluation methods. Both sides of the powder layer (+x and -x coordinates of the simulation) were studied, and the roughness values from each side were averaged to represent the surface quality. A scale factor was defined to convert pixel measurements into physical dimensions, using a reference scale from the captured images. The image of the powder bed cross-section was converted to grayscale (Figure 3a) to simplify the data while keeping the intensity information intact, and then transformed into a binary format using a threshold value of 250 to isolate the powder bed surface from the background (Figure 3b). Edges of the surface were identified using the Canny edge-detection algorithm, and these edges were overlaid on the binary image to outline the irregular surface (Figure 3c). The coordinate system was adjusted by shifting the origin to the bottom-left corner of the image to align with the physical reference frame. The highest points for each unique X-coordinate in the image were extracted to define the uppermost surface profile, and these points were sorted and scaled using the scale factor to convert the pixel data into physical dimensions. The arithmetic mean roughness (R_a) was calculated by measuring the average absolute deviation of the Y-coordinates from their mean value, and this roughness value was normalized by dividing R_a by the average particle size d_{50}, enabling meaningful comparisons across different particle size distributions. This method provides a detailed and reliable evaluation of the powder bed's surface roughness.

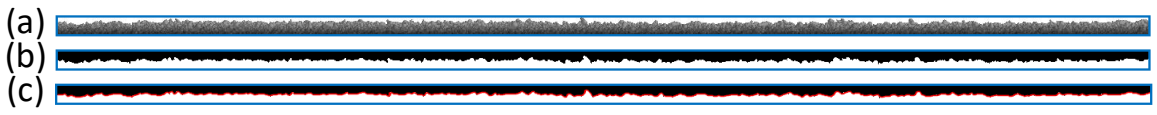

Figure 3: Image processing steps of the cross-section of obtained powder beds: (a) Grayscale image; (b) binarizing and segmentation; and (c) edge detection. Note: the blue border marks the image limits.

3. Results and Discussion

Figure 4 shows the powder layers for each spreading tool. The particles are coloured based on their height relative to the spreading gap size. In the top view of the powder layers (Figure 4a and c), more red particles indicate greater spread powder thickness. The cross-section view (Figure 4d) shows better packing and a more uniform layer with the roller-shaped tool compared to the blade-shaped tool (Figure 4b). Thus, the roller-shaped tool produced a more compact, uniform, and thicker powder layer. The results show that the spread powder layer does not fully cover the base plate to achieve a normalized height of 1 with either spreading tool at a speed of 30 mm/s. This finding may be due to the wall effect, where particles in the first layer interact with the solid metallic surface, as noted in previous studies (Chen et al., 2019).

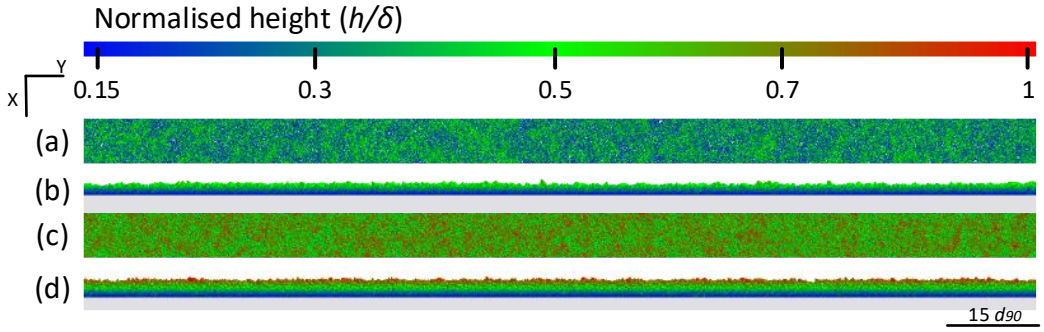

Figure 4: Powder layer spread using different tools: (a) top view with the blade-shaped tool; (b) cross-section with the blade-shaped tool; (c) top view with the roller-shaped tool; (d) cross-section with the roller-shaped tool.

Figure 5a presents the evolution of calculated packing fraction along the spreading direction, revealing clear differences between the blade and roller tools. The results show a notable shift of packing fraction profile to higher values when transitioning from the blade tool to the roller tool. This shift emphasizes the roller tool's effectiveness in better packing the powder layer, which is essential for improving the overall quality of the spread bed in PBF processes.

Coherently, the average packing fraction is significantly higher for the roller tool, reaching 0.4 compared to 0.23 for the blade tool. This increase demonstrates the roller tool's superior ability to compact the powder particles during spreading. The improved packing fraction obtained with the roller tool, compared to the blade, indicates not only a more compact layer but also the potential for a more stable base for subsequent layers (Wu et al., 2023), contributing to better final part properties (Sofia et al., 2019; Tang et al., 2023).

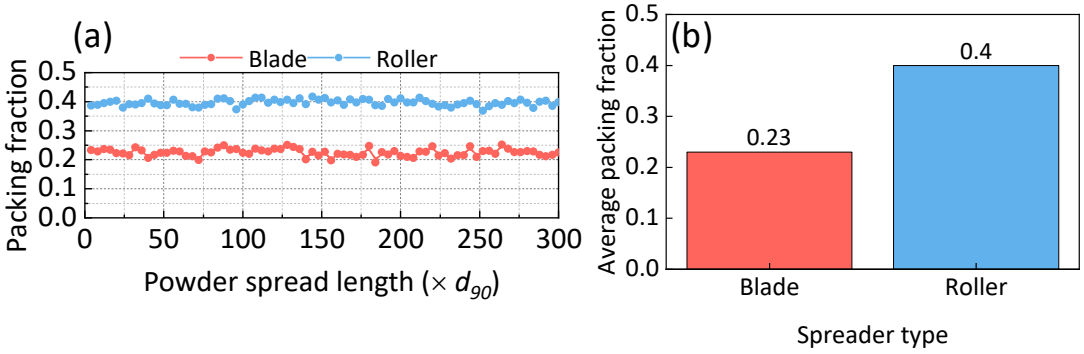

Figure 5: Packing fraction evolution along the spreading direction; (b) average packing fraction.

The surface roughness profiles of the powder layers were analyzed using image processing, as detailed in Section 2.3. Figure 6 illustrates the roughness profiles over $150d_{90}$ of the spread bed and along the -x cross-section of the simulation. The roughness profile for the blade tool shows larger fluctuations, with occasional sharp increases, indicating a less consistent surface. In contrast, the roller tool's profile is positioned higher, which reflects the greater thickness of the spread powder layer but with fewer abrupt changes.

Further analysis of the normalized surface roughness values highlights significant differences between the tools. The blade tool exhibits a higher roughness value of 0.25, suggesting a more irregular surface. In comparison, the roller tool demonstrates a lower roughness value of 0.19, indicating a smoother and more uniform surface.

These findings confirm that the roller-shaped tool achieves better surface quality and consistency in powder spreading for these irregular particles.

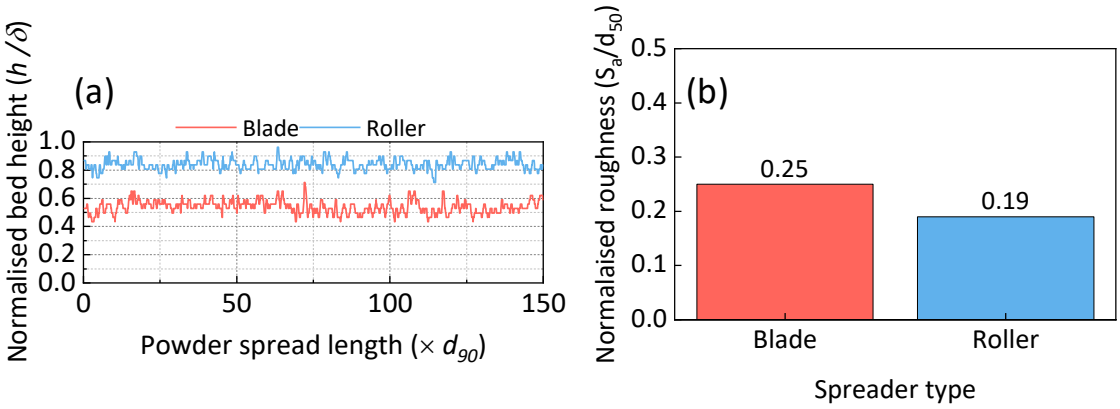

Figure 6: For the two spreading tools: (a) surface roughness profile; (b) normalised roughness values.

4. Conclusions

DEM modelling of the powder spreading step in PBF, using particles accurately representing particle shapes, enables an efficient analysis of the powder layer obtained. It also enabled the impact of the spreading tool geometry on the powder layer quality to be examined. The roller-shaped tool demonstrated superior performance compared to the blade-shaped tool, achieving higher packing fractions, lower surface roughness, and greater uniformity in the spread powder layer. These improvements are crucial for enhancing layer stability and final part quality. DEM simulations represent a tool that can guide design optimization to improve powder bed uniformity, reduce defects, and enhance the efficiency and reliability of the PBF process.

Future work will explore other spreading tool geometries, investigate higher spreading speeds to increase production rates and simulate multiple layers to replicate real systems better and mitigate wall effects. Experimental tests with roller-shaped spreaders will also be conducted to validate the simulation results more thoroughly.

References

Behjani, M.A., Rahmanian, N., Fardina bt Abdul Ghani, N., Hassanpour, A., 2017. An investigation on process of seeded granulation in a continuous drum granulator using DEM. Advanced Powder Technology 28, 2456–2464. https://doi.org/10.1016/j.apt.2017.02.011

Chen, H., Chen, Y., Liu, Y., Wei, Q., Shi, Y., Yan, W., 2020. Packing quality of powder layer during counter-rolling-type powder spreading process in additive manufacturing. Int J Mach Tools Manuf 153, 103553. https://doi.org/10.1016/j.ijmachtools.2020.103553

Chen, H., Wei, Q., Zhang, Y., Chen, F., Shi, Y., Yan, W., 2019. Powder-spreading mechanisms in powder-bed-based additive manufacturing: Experiments and computational modeling. Acta Mater 179, 158–171. https://doi.org/10.1016/j.actamat.2019.08.030

Cordova, L., Bor, T., de Smit, M., Campos, M., Tinga, T., 2020. Measuring the spreadability of pre-treated and moisturized powders for laser powder bed fusion. Addit Manuf 32, 101082. https://doi.org/10.1016/j.addma.2020.101082

Favier, J.F., Abbaspour-Fard, M.H., Kremmer, M., Raji, A.O., 1999. Shape representation of axi-symmetrical, non-spherical particles in discrete element simulation using multi-element model particles. Engineering Computations (Swansea, Wales) 16. https://doi.org/10.1108/02644409910271894

He, Y., Hassanpour, A., Bayly, A.E., 2021. Combined effect of particle size and surface cohesiveness on powder spreadability for additive manufacturing. Powder Technol 392, 191–203.

Hertz, H., 1881. Über die Berührung fester elastischer Körper. Journal für die reine und angewandte Mathematik 92, 156–171.

Horn, M., Schmitt, M., Langer, L., Schlick, G., Seidel, C., 2024. Laser powder bed fusion recoater selection guide — Comparison of resulting powder bed properties and part quality. Powder Technol 434, 119356. https://doi.org/10.1016/j.powtec.2023.119356

Johnson, K.L., Kendall, K., Roberts, A.D., 1971. Surface energy and the contact of elastic solids. Proceedings of the Royal Society of London. A. Mathematical and Physical Sciences 324, 301–313. https://doi.org/10.1098/rspa.1971.0141

Lupo, M., Sofia, D., Barletta, D., Poletto, M., 2019. Calibration of DEM Simulation of Cohesive Particles. Chem Eng Trans 74, 379–384. https://doi.org/10.3303/CET1974064

Lupo, M., Zinatlou Ajabshir, S., Sofia, D., Barletta, D., Poletto, M., 2024. Discrete element method model calibration and validation for the spreading step of the powder bed fusion process to predict the quality of the layer surface. Particuology 94, 261–273. https://doi.org/10.1016/j.partic.2024.08.010

Lupo, M., Zinatlou Ajabshir, S., Sofia, D., Barletta, D., Poletto, M., 2023. Experimental metrics of the powder layer quality in the Selective Laser Sintering process. Powder Technol 419, 118346. https://doi.org/10.1016/j.powtec.2023.118346

Mindlin, R.D., 1949. Compliance of Elastic Bodies in Contact. J Appl Mech 16, 259–268. https://doi.org/10.1115/1.4009973

Mindlin, R.D., Deresiewicz, H., 1989. Elastic Spheres in Contact Under Varying Oblique Forces, J. Applied Mech. https://doi.org/10.1007/978-1-4613-8865-4_35

Mohammadkamal, H., Caiazzo, F., 2025. Numerical Study to Analyze the Influence of Process Parameters on Temperature and Stress Field in Powder Bed Fusion of Ti-6Al-4V. Materials 18, 368. https://doi.org/10.3390/ma18020368

Mohammadkamal, H., Caiazzo, F., 2024. Influence of absorptivity variation on Laser Powder Bed Fusion simulation and impact of process parameters on residual stress formation. Procedia CIRP 124, 335–340. https://doi.org/10.1016/j.procir.2024.08.129

Nan, W., Gu, Y., 2022. Experimental investigation on the spreadability of cohesive and frictional powder. Advanced Powder Technology 33, 103466. https://doi.org/10.1016/j.apt.2022.103466

Phua, A., Doblin, C., Owen, P., Davies, C.H.J., Delaney, G.W., 2021. The effect of recoater geometry and speed on granular convection and size segregation in powder bed fusion. Powder Technol 394. https://doi.org/10.1016/j.powtec.2021.08.058

Sofia, D., Lupo, M., Barletta, D., Poletto, M., 2019. Validation of an experimental procedure to quantify the effects of powder spreadability on selective laser sintering process. Chem Eng Trans. https://doi.org/10.3303/CET1974067

Tang, M., Guo, Y., Zhang, W., Ma, H., Yang, L., Wei, W., Wang, L., Fan, S., Zhang, Q., 2023. On recoated powder quality with a forward rotating flexible roller in laser powder bed fusion of 30 wt% 5 μm SiCp/AlSi10Mg composites. Mater Des 225, 111489. https://doi.org/10.1016/j.matdes.2022.111489

Wang, L., Yu, A., Li, E., Shen, H., Zhou, Z., 2021. Effects of spreader geometry on powder spreading process in powder bed additive manufacturing. Powder Technol 384, 211–222. https://doi.org/10.1016/j.powtec.2021.02.022

Wu, S., Yang, Y., Huang, Y., Han, C., Chen, J., Xiao, Y., Li, Y., Wang, D., 2023. Study on powder particle behavior in powder spreading with discrete element method and its critical implications for binder jetting additive manufacturing processes. Virtual Phys Prototyp 18. https://doi.org/10.1080/17452759.2022.2158877

Yao, D., Wang, J., Li, M., Zhao, T., Cai, Y., An, X., Zou, R., Zhang, H., Fu, H., Yang, X., Zou, Q., 2022. Segregation of 316L stainless steel powder during spreading in selective laser melting based additive manufacturing. Powder Technol 397, 117096. https://doi.org/10.1016/j.powtec.2021.117096

Yim, S., Bian, H., Aoyagi, K., Yamanaka, K., Chiba, A., 2022. Spreading behavior of Ti–48Al–2Cr–2Nb powders in powder bed fusion additive manufacturing process: Experimental and discrete element method study. Addit Manuf 49, 102489. https://doi.org/10.1016/j.addma.2021.102489

Zhao, Y., Chew, J.W., 2021. Effect of lognormal particle size distributions on particle spreading in additive manufacturing. Advanced Powder Technology 32. https://doi.org/10.1016/j.apt.2021.02.019

Zinatlou Ajabshir, S., Hare, C., Sofia, D., Barletta, D., Poletto, M., 2024a. Investigating the effect of temperature on powder spreading behaviour in powder bed fusion additive manufacturing process by Discrete Element Method. Powder Technol 436, 119468. https://doi.org/10.1016/j.powtec.2024.119468

Zinatlou Ajabshir, S., Sofia, D., Hare, C., Barletta, D., Poletto, M., 2024b. Experimental characterisation of the spreading of polymeric powders in powder bed fusion additive manufacturing process at changing temperature conditions. Advanced Powder Technology 35, 104412. https://doi.org/10.1016/j.apt.2024.104412